Locally Weighted Multi-atlas Construction

Junning Li, Yonggang Shi, Ivo D. Dinov, and Arthur W. Toga*

Laboratory of Neuro Imaging, Department of Neurology
University of California, Los Angeles, CA, USA
{junningl,yonggang.shi}@gmail.com, dinov@ucla.edu, toga@usc.edu

Abstract. In image-based medical research, atlases are widely used in many tasks, for example, spatial normalization and segmentation. If atlases are regarded as representative patterns for a population of images, then multiple atlases are required for a heterogeneous population. In conventional atlas construction methods, the "unit" of representative patterns is images. Every input image is associated with its most similar atlas. As the number of subjects increases, the heterogeneity increases accordingly, and a big number of atlases may be needed. In this paper, we explore using region-wise, instead of image-wise, patterns to represent a population. Different parts of an input image is fuzzily associated with different atlases according to voxel-level association weights. In this way, regional structure patterns from different atlases can be combined together. Based on this model, we design a variational framework for multi-atlas construction. In the application to two T1-weighted MRI data sets, the method shows promising performance, in comparison with a conventional unbiased atlas construction method.

1 Introduction

In image-based medical researches, atlases are widely used to represent a population of images. They provide common spaces for spatial normalization, references for alignment, and propagation sources for segmentation.

One of the most widely used methods is registering input images to a preselected reference image, and then taking the average of the warped images as the atlas. Because all the images are transformed to be as similar as possible to the reference, the choice of the reference has significant impacts on the result. To avoid the bias introduced by arbitrary choice, the average image or the geometric mean of the input images can be used as the initial reference, as proposed by Joshi et al. (2004) [1] and Park et al. (2005) [2]. Instead of transforming input images toward a reference image, Seghers et al. (2004) [3] transformed them with the morphological mean of their transformations to all the other images. This method requires registration between all input image pairs.

In recent years, manifold-guided group registration methods are developed. Relationship between the input images is modeled with a manifold, and the input images are transformed gradually along the manifold to a center, instead of

* This work is supported by grants K01EB013633, R01MH094343, and P41EB015922 from NIH.

L. Shen et al. (Eds.): MBIA 2013, LNCS 8159, pp. 1–8, 2013.

directly "jump" to a reference image. This avoids inaccurate direct registration between dissimilar images. The manifold is usually represented by a k-nearest-neighbor graph whose vertices represent images and whose edges are weighted with the transformational metric between two images. Hamm et al. (2010) [4] employed the minimum spanning tree of the graph to guide the registration. Jia et al. (2010) [5] and Wang et al. (2010) [6] embedded a clustering procedure to merge images as intermediate centers when they become similar enough. Such a method not only reduces computation load but also builds a hierarchical structure for the inputs. Wu et al. (2011) [7] used directed graphs instead of undirected ones to optimize the registration procedure.

For a heterogeneous population, multiple atlases are required to represent it, as discussed in [8] by Blezek and Miller. Multi-atlases are usually constructed by partitioning the input images into sub-groups and then constructing an atlas for each of them. Aljabar et al. (2009) showed that the way of partitioning considerably impacts the result. Therefore, data-driven approaches should be employed. Sabuncu et al. (2009) [9] used Gaussian mixture models to cluster input images. Xie et al. (2013) [10] clustered input images according the manifold formed by them.

If atlases are regarded as representative patterns for a population of images, the "unit" of patterns used in the aforementioned methods is images. Every input image is associated with its most similar atlas. As the number of subjects increases, the heterogeneity among subjects increases accordingly. To represent a large population, we may need a big number of atlases. Let us assume the following not rigorously correct yet illustrating situation. Suppose the brain has m anatomic structures, and each structure has n possible patterns among a population. To represent all the possible combinations, we may need $m \times n$ atlases, if the pattern unit is images.

In this paper, we explore using region-wise, instead of image-wise, patterns to represent a population of images. We allow different parts of an input image to fuzzily associate with different atlases according to voxel-level association weights. In this way, structure patterns from different atlases can be combined together. In Section 2, we present a variational framework for constructing such a locally weighted multi-atlas. In Section 3, we demonstrate its application to two T1-weighted MRI data sets, where the proposed method show promising performance, in comparison with the group-mean method [1]. In Section 4, we briefly discuss possible future work.

2 Locally Weighted Multi-atlas

2.1 Generative Model

We assume that the input images are generated with voxel-level random sampling from a small number of template images and then they are randomly warped. Such a generative model is illustrated in Fig. 1 and the notations used in it is listed in Table 1. In the template space, the intensity value at point x of a latent image $\bar{I}_s$ is randomly sampled from template images $\{T_k, k = 1, \ldots, K\}$, at the same point

Table 1. Notations

I_s	Image of subject s	T_k	The kth atlas image
φ_s	Transformation for image I_s	x	Point in space
$\hat{I}_s = I_s \circ \varphi_s$	Warped image of subject s	$W_{sk}(x)$	Weight of $\bar{I}_s(x)$'s association with T_k
$\bar{I}_s$	Latent image of $\hat{I}_s$	Ω	Spatial domain

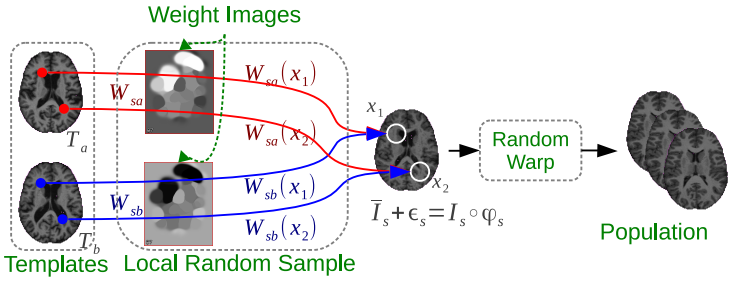

Fig. 1. Generative Model

location, where K is the number of atlases. After noise ε_s is added to it, $\bar{I}_s$ is randomly warped to be an input image I_s. The voxel-level probability distribution that intensity values of $\bar{I}_s$ are sampled from T_ks is configured with weight images $\{W_{sk}, k = 1, \ldots, K|s\}$. Such a generative process can be written as

$$\kappa_s(x) \sim \text{Multinomial}\{W_{sk}(x), k = 1, \ldots, K|s\} \tag{1}$$

$$\bar{I}_s(x) = T_{\kappa_s(x)}(x) \tag{2}$$

$$I_s = (\bar{I}_s + \varepsilon_s) \circ \varphi_s^{-1} \tag{3}$$

where Multinomial$\{W_{sk}(x), k = 1, \ldots, K|s\}$ denotes a multinomial distribution such that $P(\kappa = k) = W_{sk}(x)$ and $\{W_{sk}, k = 1, \ldots, K|s\}$ satisfies $\sum_k W_{sk}(x) = 1$ for any s and x.

The intensity values of $\bar{I}_s$ at different points can be sampled from different template images. In this way, $\bar{I}_s$ is able to combine different patterns from different templates. To avoid abrupt transition between structure patterns, adjacent points should intend to be sampled from the same template image, and the weight images W_{sk} should be spatially smooth.

Fig. 2 shows an example of such a generative process. Each of the images is composed of two parts, one from the images of either letter "A" or letter "B", the other from the images of either letter "C" or letter "D". In total, there are four image-level patterns: "AB", "AD", "CB" and "CD", as shown in the middle row of figure. Then the four patterns are randomly warped to be input images, as

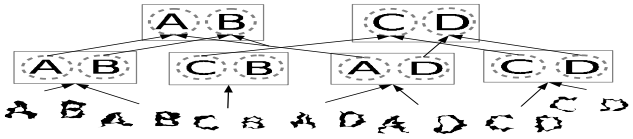

Fig. 2. Example of Image Generation Process

shown in the bottom row of the figure. If we represent the images with regional patterns, we just need two atlases: "AB" and "CD" (as shown in the top row of the figure), or "AD" and "CB", instead four atlases.

2.2 Atlas Construction Model

Based on the generative model defined in Eqs. (1), (2) and (3), we design the following energy function for locally weighted multi-atlas construction:

$$J = J_{\text{sim}} + J_{\text{cls}} + J_{\text{trans}} + J_{\text{wt}} \tag{4}$$

where J_{sim} counts for image similarity in the template space, J_{cls} for clustering dispersion, J_{trans} for transformation smoothness, and J_{wt} for weight image smoothness.

J_{sim} is defined as

$$J_{\text{sim}} = \sum_s \int_{x\in\Omega} \sum_k W_{sk}(x) \left\| I_s \circ \varphi_s(x) - T_k(x) \right\|^2 dx \tag{5}$$

where the weight images satisfy $W_{sk}(x) \geqslant 0$ and $\sum_k W_{sk}(x) = 1$ for any s and x.

J_{cls} is defined as

$$J_{\text{cls}} = \sum_s \int_{x\in\Omega} h(x) \sum_k W_{sk}(x) \ln \frac{W_{sk}(x)}{Q_k(x)} dx \tag{6}$$

where $\{Q_k, k = 1, \ldots, K\}$ are prior weight images and $h(x)$ is a penalty factor. Being the integration of the Kullback–Leibler divergence between $\{W_{sk}\}$ and $\{Q_k\}$, J_{cls} imposes similarity between $\{W_{sk}\}$ and $\{Q_k\}$. For simplicity, we used $Q_k(x) = 1/K$.

J_{wt} is defined as

$$J_{\text{wt}} = \sum_s \int_{x\in\Omega} \sum_k \langle \nabla W_{sk}, \nabla W_{sk} \rangle \, dx \tag{7}$$

to model the smoothness of the weight images.

J_{trans} is defined as

$$J_{\text{trans}} = \sum_s \int_{x\in\Omega} \langle D\varphi_s, D\varphi_s \rangle \, dx \tag{8}$$

where D is a spatial difference operator. For diffusion regularization, D is the gradient operator; for curvature regularization, D is the Laplace operator.

2.3 Alternating Optimization

The energy function defined in Section 2.2 involves the following parameters: the transformations φ_s, the template images T_k, and the weight images W_{sk} . For simplicity, we do to treat the penalty factor $h(x)$ as a parameter to optimize, but as a given configuration of the energy function. Though a large number of parameters are involved in the energy function, they can be solved one by one with alternating optimization.

2.3.1 Optimizing T_k Given φ_s and W_{sk}: T_k is involved only in J_{sim}, as the center of weighted variances, as shown in Eq. (5). Given φ_s and W_{sk}, the optimal value of T_k is the locally weighed average of $I_s \circ \varphi_s$, as defined in the following equation:

$$T_k(x) = \frac{\sum_s W_{sk}(x) \times I_s \circ \varphi_{sk}(x)}{\sum_s W_{sk}(x)}$$

2.3.2 Optimizing W_{sk} Given T_k and φ_s: W_{sk} is involved in J_{sim}, J_{cls} and J_{wt}. Because J_{wt} imposes smoothness on W_{sk} and its Green's function is a Gaussian kernel, for simplicity, we first solve W_{sk} with J_{sim} and J_{cls}, and then smooth it with a Gaussian kernel. The method of Lagrange multipliers implies that to minimize J_{sim} and J_{cls} under the constraint $\sum_k W_{sk}(x) = 1$, W_{sk} must satisfy

$$W_{sk}(x) \propto U_{sk}(x) := Q_k(x) e^{-\frac{\|I_s \circ \varphi_s(x) - T_k(x)\|^2}{h(x)}}$$

Therefore, the solution of $W_{sk}(x)$ without smoothing is $\frac{U_{sk}(x)}{\sum U_{sk}(x)}$.

2.3.3 Optimizing φ_s Given T_k and W_{sk}: φ_s is involved in J_{sim}, and J_{trans}. The contribution of a particular φ_s to the total energy function J is

$$\begin{aligned} J_{\varphi_s} = & \int_{x\in\Omega} \sum_k W_{sk}(x) \|I_s \circ \varphi_s(x) - T_k(x)\|^2 \, dx + \int_{x\in\Omega} \langle D\varphi_s, D\varphi_s \rangle \, dx \\ = & \int_{x\in\Omega} \left\| I_s \circ \varphi_s(x) - \sum_k W_{sk}(x) T_k(x) \right\|^2 dx + C + \int_{x\in\Omega} \langle D\varphi_s, D\varphi_s \rangle \, dx \end{aligned}$$

where C is a constant fully determined by T_k and W_{sk}. As the equation implies, φ_s can be optimized by registering I_s to $\sum_k W_{sk} T_k$.

3 Experiments

The proposed method is applied to one synthetic data set (100 images) and two real MRI data sets (each of 40 images) for atlas construction, and compared with the conventional unbiased group-mean method [1]. The group-mean method registers input images to the average of their warped images, and iteratively repeats this procedure. Before atlas construction, we linearly align all the input images. For multi-atlas construction, we set the number of atlases K to two.

The Dice label overlap index is used to measure the performance of the methods. The template label images L_ks are derived from the warped input label images, with weighted majority vote according to weights $\{W_{sk}, s = 1, \ldots, S|k\}$. The predicted label image for a warped image $\hat{I}_s$ in the template space, is derived from the template label images by fusing them together with weighted majority vote according to weights $\{W_{sk}(x), k = 1, \ldots, K|s\}$.

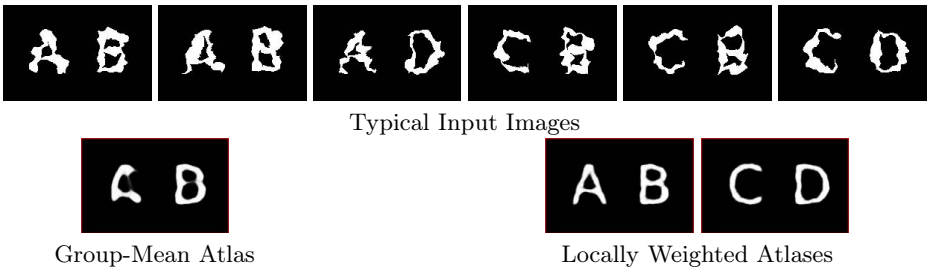

Fig. 3. ABCD100

3.1 Synthetic Data

We generate 100 images according the model illustrated in Figs. 1 and 2. For the description of the generative procedure, please refer to Section 2.1. We expect the proposed method to recover the underlying region-level patterns "A", "B", "C", "D" as two atlas images, for example "AB" and "CD", or "AD" and "CB", instead using four atlases. As shown in Fig. 3, the proposed method satisfactorily recovers the underlying regional patterns as two images "AB" and "CD".

3.2 OASIS Data Set

The OASIS data set contains T1-weighted MR brain images of 416 subjects at ages ranging from 18 to 96. The images are at the resolution of $1 \times 1 \times 1$ mm^3 and of voxel size 176×208×176. For each subject, a label image indicating the segmentation of white matter (WM), gray matter (GM) and cerebrospinal fluid (CSF) is also provided. We randomly sampled 40 images from the data set, one half with ages ranging from 20 to 30, and the other half ranging from 70 to 80.

As shown in Fig. 4, the proposed method constructs one atlas with a large ventricle and the other with a smaller one. The proposed method achieves better tissue overlap than the group-mean method (86.9% vs. 81.4%), as shown in the table in Fig. 4.

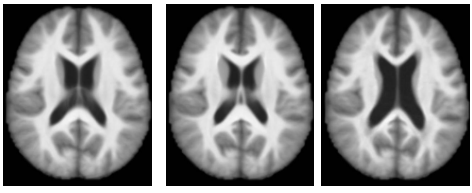

	Overall	CSF	GM	WM
Group-Mean	81.4	64.9	84.3	84.5
LWM	86.9	74.4	88.1	91.2

Dice Indices of Tissue Overlap

Fig. 4. OASIS40. "LWM" means locally weighted multi-atlas.

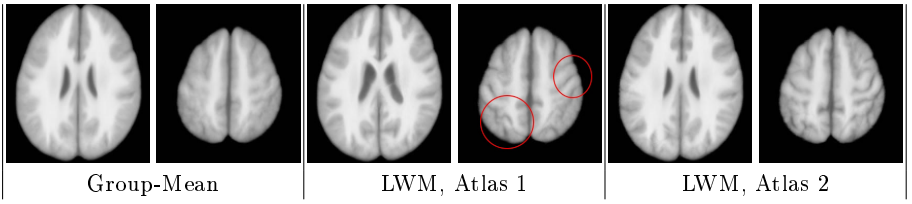

Fig. 5. LPBA40: Constructed Atlases. "LWM" means locally weighted multi-atlas.

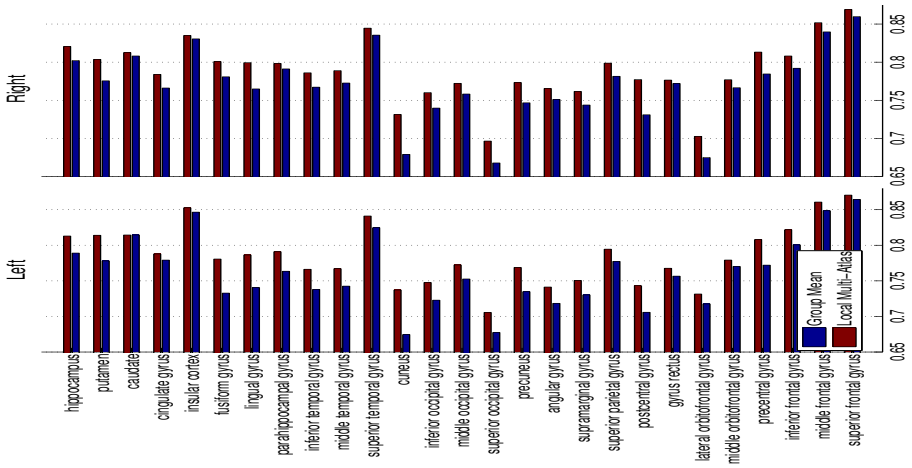

Fig. 6. LPBA40: Dice Overlap Indices of 54 ROIs

3.3 LPBA40 Data Set

The LPBA40 data set [11] has T1 images of 40 subjects and 54 regions are manually segmented for each of them. The proposed method is applied to it, with the number of atlases K set to two. As shown in Fig. 5, the two atlases produced by the proposed method show different patterns in the upper part of the brain, and are visually sharper than that by the group-mean method. The overall Dice overlap indices of the proposed method and the group-mean method are 80.4% and 78.5% respectively. Overlap indices of the 54 regions are shown in Fig. 6.

4 Conclusion and Discussion

In this paper, we exploring using region-wise, instead of image-wise, patterns to represent a population of images. Different parts of an input image are fuzzily associated with different atlases according to voxel-level association weights. In this way, structure patterns in different atlases can be combined together. Such a

model can be formulated in a variational framework for multi-atlas construction, and solved with alternating optimization. In the applications to the OASIS and LPBA40 data sets, the proposed method achieves better label overlap than the conventional group-mean method [1].

It worths further investigation to use morphological difference, instead of intensity difference, for determining the voxel-level association weights. Choosing an appropriate number of atlases is another interesting topic for future study.

References

1. Joshi, S., Davis, B., Jomier, M., Gerig, G.: Unbiased diffeomorphic atlas construction for computational anatomy. NeuroImage 23(Suppl. 1), S151–S160 (2004)
2. Park, H., Bland, P.H., Hero III, A.O., Meyer, C.R.: Least biased target selection in probabilistic atlas construction. In: Duncan, J.S., Gerig, G. (eds.) MICCAI 2005. LNCS, vol. 3750, pp. 419–426. Springer, Heidelberg (2005)
3. Seghers, D., D'Agostino, E., Maes, F., Vandermeulen, D., Suetens, P.: Construction of a brain template from Mr images using state-of-the-art registration and segmentation techniques. In: Barillot, C., Haynor, D.R., Hellier, P. (eds.) MICCAI 2004. LNCS, vol. 3216, pp. 696–703. Springer, Heidelberg (2004)
4. Hamm, J., Ye, D.H., Verma, R., Davatzikos, C.: Gram: A framework for geodesic registration on anatomical manifolds. Med. Image Anal. 14(5), 633–642 (2010)
5. Jia, H., Wu, G., Wang, Q., Shen, D.: Absorb: Atlas building by self-organized registration and bundling. Neuroimage 51(3), 1057–1070 (2010)
6. Wang, Q., Chen, L., Yap, P.-T., Wu, G., Shen, D.: Groupwise registration based on hierarchical image clustering and atlas synthesis. Hum. Brain Mapp. 31(8), 1128–1140 (2010)
7. Wu, G., Jia, H., Wang, Q., Shen, D.: Sharpmean: groupwise registration guided by sharp mean image and tree-based registration. Neuroimage 56(4), 1968–1981 (2011)
8. Blezek, D.J., Miller, J.V.: Atlas stratification. Med. Image Anal. 11(5), 443–457 (2007)
9. Sabuncu, M.R., Balci, S.K., Shenton, M.E., Golland, P.: Image-driven population analysis through mixture modeling. IEEE Transactions on Medical Imaging 28(9), 1473–1487 (2009)
10. Xie, Y., Ho, J., Vemuri, B.: Multiple atlas construction from a heterogeneous brain MR image collection. IEEE Transactions on Medical Imaging PP(99), 1 (2013)
11. Shattuck, D.W., Mirza, M., Adisetiyo, V., Hojatkashani, C., Salamon, G., Narr, K.L., Poldrack, R.A., Bilder, R.M., Toga, A.W.: Construction of a 3D probabilistic atlas of human cortical structures. Neuroimage 39(3), 1064–1080 (2008)